J. Hydrol. Hydromech., 67, 2019, 4, 329–338
DOI: 10.2478/johh-2019-0022

Submergence coefficient of full-width sharp-edged broad-crested rectangular weirs

Zbyněk Zachoval[1*], Jakub Major[1], Ladislav Roušar[2], Ján Rumann[3], Jan Šulc[1], Jan Jandora[1]

[1] Brno University of Technology, Faculty of Civil Engineering, Institute of Water Structures, Veveří 331/95, 602 00 Brno, Czech Republic.
[2] VHRoušar, Radčice 24, 539 73 Skuteč, Czech Republic.
[3] Slovak University of Technology in Bratislava, Faculty of Civil Engineering, Department of Hydraulic Engineering, Radlinského 11, 810 05 Bratislava, Slovak Republic.
[*] Corresponding author. E-mail: zachoval.z@fce.vutbr.cz

Abstract: Full-width sharp-edged broad-crested rectangular weirs in the range $0.1 < h/L \leq 0.3$ situated in rectangular channels are frequently used in submerged flow conditions. To determine the discharge for the submerged flow, submergence coefficient and modular limit shall be known. This article deals with their determination upon a theoretic derivation and experimental research. The equation for modular limit has been determined from energy balance with simplifications. To validate it, extensive experimental research was carried out. However, the derived equation is too complicated for practical use which is why it was approximated by a simple equation applicable for the limited range. The equation for submergence coefficient was derived by modifying Villemonte's application of the principle of superposition and its coefficients were determined using the data from experimental research of many authors. The new system of equations computes the discharge more accurately than other authors' equations, with the error of approximately ±10% in full range of the measured data.

Keywords: Modular limit; Relative weir height; Full-width sharp-edged broad-crested weir; Submergence coefficient.

INTRODUCTION

According to the length of weir in direction of flow, L, weirs of finite-crest width for free flow are classified as (Govinda Rao and Muralidhar, 1963): long-crested weirs $0.0 < h/L \leq 0.1$, broad-crested weirs $0.1 < h/L \leq 0.4$, short-crested weirs $0.4 < h/L \leq 1.5$ to 1.9, and sharp-crested weirs 1.5 to $1.9 < h/L$, where h is the upstream head over the weir crest (Fig. 1). In the text below, broad-crested weirs with sharp (square) upstream and downstream edges, with rectangular longitudinal and cross section profiles in the range $0.1 < h/L \leq 0.3$ are considered. In this range the parallel flow will occur on the weir crest (Bos, 1989) and discharge coefficient for free flow is in effect independent of h/L (Zachoval et al. 2014a). Many authors carried out experimental research with free overflow to determine the discharge coefficient (Azimi et al., 2014; Bazin, 1896; Berezinsky, 1950; Crabbe, 1974; Doeringsfeld and Barker, 1941; Goodarzi et al., 2012; Hager and Schwalt, 1994; Kašpar, 2015; Keutner, 1934; Madadi et al., 2014; Major, 2013; Prentice, 1941 (in Stevens et al., 1941); Rafter, 1900; Sahasrabudhe, 1972; Singer, 1964; Sreetharan, 1983, Tim, 1986; Woodburn, 1932; Zachoval et. al., 2014a) and many authors determine it theoretically (Pavlovsky, 1937; Skogerboe et al., 1967; Tim, 1986).

Sharp-edged broad-crested rectangular weirs are usually designed and operated in submerged flow conditions. One of their biggest advantages compared to other weir types is the high value of modular limit (Bos, 1989), which is the state on the boundary of free and submerged flow. Submerged flow may appear on weirs with little difference between the water levels, especially in extreme discharge conditions. To determine the discharge for submerged flow, submergence coefficient (drowned flow-reduction factor) which corrects the discharge value compared to the free flow shall be known.

In the case of relatively high sharp-edged broad-crested weirs, where the discharge coefficient and the submergence coefficient are basically independent of relative weir height above the channel bed, the information on modular limit and the submergence coefficient are described well (Bos, 1989; Pavlovsky, 1937; USACE, 1977). As for the relatively low weirs, where the modular limit and the submergence coefficient are greatly affected by relative weir height, the information is less detailed and considerably differs. It is one of the reasons why many authors do not recommend measuring of the discharge in submerged flow conditions (Bos, 1984; Hager, 2010; Hager and Schwalt, 1994; Horton, 1907). Due to the above fact, extensive research was carried out focusing on determination of the modular limit and submergence coefficient for a full-width sharp-edged broad-crested rectangular weir in the ranges of $0.1 < h/L \leq 0.3$ and $0.1 < h/P < 3.0$, where P is the weir height.

LITERATURE REVIEW

In the long term, the submerged flow was dealt with by a large number of researchers whose summary is listed e.g. by Horton (1907) and Skogerboe et al. (1967). The studies mostly focused on thin-plate weirs. A substantially lower number of researches concentrated on rectangular short-crested (Azimi et al., 2014) and broad-crested weirs.

For flows over broad-crested weirs, modular limit used to be determined, less often the submergence coefficient. An extensive experimental research on modular limit of round-nosed broad-crested weirs was published by Woodburn (1932). Modular limit and submergence coefficients of various broad-crested weir types were experimentally studied by Berezinskij (1950). Skogerboe et al. (1967) derived an equation for calculation of discharge for submerged flow from the momentum analysis of flow. Harrison (1967) derived modular limit for weirs with round-nosed upstream corner of crest depending on relative weir height above the outflow channel bed. Sahasrabudhe (1972) carried out experimental research on determination of submergence coefficient for round and sharp upstream edge of the weir crest. USACE (1977) recommended graphical de-

pendence to determine the submergence coefficient. Nikolov et al. (1978) summed up and particularized recommendations for calculation of submergence coefficient. Bos (1984) recommends determination of modular limit upon mechanical energy analysis. Tim (1986) performed measurements with the stress laid on the effect of the rounding of upstream edge on the submergence coefficient. Hager and Schwalt (1994) determined modular limit through an experiment and expressed the submergence coefficient by means of the index of the tailwater flow depth $\chi = (h_f - h_{f0})/(H - h_{f0})$, where h_f is the submergence head, H is the total head and h_{f0} is the submergence head for modular limit. Bukreev (2001) studied flow over a submerged weir of relatively small height. Wols (2005) carried out experimental research focusing on the measurement of water level and defined the submergence coefficient upon the Villemonte's analysis under submerged flow conditions (Villemonte, 1947). ISO 3846 (2008) recommended determination of modular limit and submergence coefficient solely for the specific weir geometry. Azimi et al. (2014) defined modular limit and submergence coefficient on the basis of their measurements. Geometric parameters and ranges of experimental research of the above listed authors are shown in Table 1. In spite of the rather extensive number of researches into the issue, the results are ambiguous and the values of modular limit and submergence coefficient have not been determined and verified for the entire applicable scope of geometric layouts (h/P), which is the subject of the research carried out by authors of this article.

HEAD-DISCHARGE RELATIONSHIP

Subscripts at quantities in the text below specify affiliation with the U, C, T, E, D profile (Fig. 1) or to a section specified by the profiles. The "0" subscript indicates modular limit conditions.

Full-width sharp-edged broad-crested rectangular weir in a horizontal channel of rectangular cross-section (ISO 3846, 2008) is considered. P_U is the upstream weir height, P_D the downstream weir height and b the weir width. The flow is caused by gravitational acceleration g and is characterised by total head over the weir H in the U profile (Fig. 1)

$$H = h + \frac{\alpha_U \cdot Q^2}{2 \cdot g \cdot b^2 \cdot \left(h + P_U\right)^2} \tag{1}$$

and the submergence total head H_f in the D profile (Fig. 1)

$$H_f = h_f + \frac{\alpha_D \cdot Q^2}{2 \cdot g \cdot b^2 \cdot \left(h_f + P_D\right)^2}, \tag{2}$$

where h is the head over the weir, h_f is the submergence head, α_U and α_D are kinetic energy coefficients (Coriolis coefficient) in profiles U and D and Q is the discharge. The U profile is situated 3h to 4h (ISO 3846, 2008) in front of the upstream face of the weir where the drawdown curve caused by the overflow is negligible. The D profile is located 10h (ISO 3846, 2008) behind the downstream face of the weir where the water level is not affected by the overflow. Measurements show that kinetic energy coefficient varies between $1.02 < \alpha_U < 1.06$ (Zachoval et al., 2012b) and $\alpha_D = 1.11$ (Zubík, 2006).

The equation for Q is derived from Bernoulli's equation for the above profiles and from the continuity equation

$$Q = C_f \cdot C_d \cdot \left(\frac{2}{3}\right)^{3/2} \cdot g^{1/2} \cdot b \cdot H^{3/2}, \tag{3}$$

where C_f is the submergence coefficient and C_d the discharge coefficient. C_f expresses reduction of the flow due to submergence, C_d expresses energy loss for free overflow. As H cannot be directly measured, the following equation is recommended to define Q

$$Q = C_f \cdot C_v \cdot C_d \cdot \left(\frac{2}{3}\right)^{3/2} \cdot g^{1/2} \cdot b \cdot h^{3/2}, \tag{4}$$

where $C_v = (H/h)^{3/2}$ is the approach velocity coefficient to be determined iteratively or read from the relation $C_v = f\{\alpha_U^{1/2} \cdot C_d \cdot h/(h + P_U)\}$ presented by Bos (1989, Figure 1.12).

Modular limit

Modular limit can be expressed by the ratio of h/h_{f0} or H/H_{f0} (Harrison, 1967). The modular limit may be determined experimentally (Azimi et al., 2014; Berezinskij, 1950; Tim, 1986), numerically (Wols, 2005) and analytically. Present analytic derivations are only known for weirs where critical flow

Table 1. Geometry and range of flow parameters.

Author	h (m)	L (m)	P (m)	b (m)	h/L	h/P	h/b
Azimi et al. (2014)	0.030–0.139	0.076–0.304	0.076	0.400	0.11–1.83	0.39–1.83	0.07–0.35
Berezinsky (1950)	0.060–0.101	0.500	0.107	0.900	0.12–0.20	0.56–0.94	0.07–0.11
Hager and Schwalt (1994)	0.030–0.181	0.500	0.401	0.499	0.06–0.37	0.07–0.45	0.06–0.36
Halliwell and Hill (1967) from Markland et al. (1967)	0.040–0.079	0.229–0.457	0.038–0.152	0.284	0.09–0.34	0.27–1.90	0.14–0.28
Sahasrabudhe (1972)	0.060–0.603	0.15–0.30	0.151–0.308	0.460	0.21–3.09	0.21–3.93	0.13–1.31
Tim (1986)	0.031–0.122	0.305	0.102	0.254	0.10–0.40	0.305–1.20	0.12–0.48
Wols (2005)	0.134–0.187	1.00	0.150	0.4	0.134–0.187	0.89–1.25	0.34–0.47

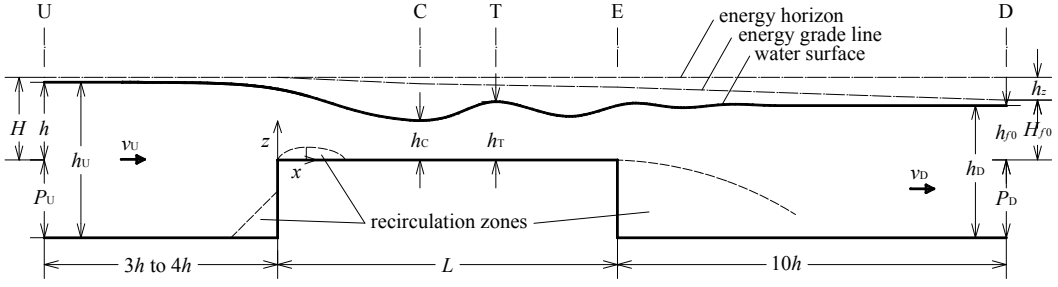

Fig. 1. Longitudinal profile of weir at modular limit.

appears along the whole crest length (rounded or bevelled upstream edge) and are based on mechanical energy analysis (Bos, 1984) and momentum analysis (Harrison, 1967). However, flow separation zone (Zachoval et al., 2012a) and undular hydraulic jump (Hager and Schwalt, 1994) form on weir crest, which is why the above analytic derivations are unsuitable and provide incorrect results.

The new analytic derivation respecting the flow separation zone and the hydraulic jump on weir crest is based on energy balance at modular limit (Fig. 1). The derivation neglects the effect of surface tension and effect of friction on side hydraulically smooth walls, which – in the case of free flow – means $h \geq 0.06$ m and $h/b \leq 0.5$ (Zachoval, 2015). To define the specific discharge q, Equation (3) is then applied

$$q = v_i \cdot h_i = \frac{Q}{b} = C_d \cdot \left(\frac{2}{3}\right)^{3/2} \cdot g^{1/2} \cdot H^{3/2}, \quad (5)$$

where v_i and h_i are mean velocity and depth in the profile i = U, C, T, E, D (Fig. 1). Total head loss is calculated as a sum of individual head losses under the presumption they do not affect one another. To determine them, profiles are defined: C which is 2.7H behind the upstream edge of weir crest where flow is contracted (Zachoval et al., 2012a); T at peak of the first wave of undular hydraulic jump; and E at the downstream edge of the weir crest.

Between the U and C profiles, the head loss h_{zUC} appears for free flow. Due to the formation of flow recirculation zone whose height and length partly depends on the H/P_U ratio (Zachoval et al., 2012a), it is to be defined from the depth h_C (in C profile) where the flow is approximately parallel. After Equation (5) is applied, the head loss in free flow conditions is

$$h_{zUC} = H - h_C - \frac{\alpha_C \cdot q^2}{2 \cdot g \cdot h_C^2} = H - h_C - \frac{2^2}{3^3} \cdot \alpha_C \cdot C_d^2 \cdot \left(\frac{H}{h_C}\right)^2 \cdot H, \quad (6)$$

where α_C is kinetic energy coefficient in profile C.

Between the C and E profiles, head loss from undular hydraulic jump, h_{zCT}, and head loss caused by friction on weir crest, h_{zCE}, appear. Expression of the head loss respecting concurrently the friction loss and the hydraulic jump loss for Froude number $Fr_C = v_C/(g \cdot h_C)^{1/2} > 2$ is known and verified (Noor Afzal et al., 2011) but not for the undular hydraulic jump on the crest of broad-crested weir where Froude number varies in the range $1.26 < Fr_C < 1.43$ ($0.1 < h/P_U < 3$). Summary information about undular hydraulic jump is described by Chanson (2009) and Montes and Chanson (1998). Information about wave profile of undular jump on the smooth crest is described by Berezinsky (1950), Bukreev (2001), Hager and Schwalt (1994) and Wols (2005). Due to the difficulty to describe the loss on the crest and the relatively low significance of the total loss (Fig. 6), the assumption of hydrostatic pressure distribution was presumed. Two simplified separate formulas have been used. The head loss caused solely by the hydraulic jump is

$$h_{zCT} = \frac{(h_T - h_C)^3}{4 \cdot h_C \cdot h_T}, \quad (7)$$

where water depth, h_T, is determined from flow momentum analysis. After Equation (5) is applied, the equation for depth is

$$h_T = \frac{h_C}{2} \cdot \left[\left(1 + 8 \cdot \frac{q^2}{h_C^3 \cdot g}\right)^{1/2} - 1\right] = \frac{h_C}{2} \cdot \left\{\left[1 + \frac{2^6}{3^3} \cdot C_d^2 \cdot \left(\frac{H}{h_C}\right)^3\right]^{1/2} - 1\right\}. \quad (8)$$

After Equation (8) is used in Equation (7), head loss caused solely by hydraulic jump can be expressed

$$h_{zCT} = \frac{\left\{\left[1 + \frac{2^6}{3^3} \cdot C_d^2 \cdot \left(\frac{H}{h_C}\right)^3\right]^{1/2} - 3\right\}^3}{2^4 \cdot \left\{\left[1 + \frac{2^6}{3^3} \cdot C_d^2 \cdot \left(\frac{H}{h_C}\right)^3\right]^{1/2} - 1\right\}} \cdot h_C. \quad (9)$$

Head loss by friction on weir crest, h_{zCE}, appears along the $L_{CE} = L - 2.7 \cdot H$ length. In effect, friction does not occur at the distance up to 2.7H, as there is a wake. As one to three waves of hydraulic jump form on the weir crest and the individual loss has rather low significance for the total loss (Fig. 6), mean depth of the flow, h_{CE}, at uniform flow is used for simplified expression of h_{zCE}. After the substitution in Equation (8)

$$h_{CE} = \frac{h_C + h_T}{2} = \frac{1}{2^2} \cdot \left\{\left[1 + \frac{2^6}{3^3} \cdot C_d^2 \cdot \left(\frac{H}{h_C}\right)^3\right]^{1/2} + 1\right\} \cdot h_C. \quad (10)$$

After applying Equation (5), mechanic energy gradient, i_{CE}, for uniform, fully turbulent flow is determined from the equation (García, 2008)

$$i_{CE} = \left(\frac{k_{sCE}}{h_{CE}}\right)^{1/3} \cdot \left(\frac{v_{CE}^2}{C_k^2 \cdot g \cdot h_{CE}}\right) = \left(\frac{k_{sCE}}{h_{CE}}\right)^{1/3} \cdot \left(\frac{q^2}{C_k^2 \cdot g \cdot h_{CE}^3}\right), \quad (11)$$

where k_{sCE} is hydraulic roughness of weir crest surface, v_{CE} the mean velocity and C_k the coefficient of proportionality (Brownlie, 1981). Head loss by friction on weir crest, h_{zCE}, after substitution of Equations (11) and (5) is then

$$h_{zCE} = i_{CE} \cdot L_{CE} = \left(\frac{2}{3}\right)^3 \cdot \left(\frac{C_d}{C_k}\right)^2 \cdot \left(\frac{k_{sCE}}{h_{CE}}\right)^{1/3} \cdot \left(\frac{H}{h_{CE}}\right)^3 \cdot (L - 2.7 \cdot H). \quad (12)$$

In profile E, the head loss is caused by sudden expansion of cross section, h_{zE}, which, assuming an idealised uniform flow in outflow channel and after Equation (5) is applied, results in

$$h_{zE} = \xi_E \cdot \left(\frac{h_D}{h_T} - 1\right)^2 \cdot \frac{q^2}{2 \cdot g \cdot h_D^2} = \frac{2^2}{3^3} \cdot \alpha_D \cdot C_d^2 \cdot \xi_E \cdot \left(\frac{H}{h_D}\right)^2 \cdot \left(\frac{h_D}{h_T} - 1\right)^2 \cdot H, \quad (13)$$

where h_D is the depth in profile D and ξ_E the minor loss coefficient for vertical downstream weir face.

Between profiles E and D, the head loss h_{zED} is caused by friction. Under the presumption of idealised uniform flow in outflow channel and after Equation (5) is applied

$$h_{zED} = \left(\frac{2}{3}\right)^{3/2} \cdot \left(\frac{C_d}{C_k}\right)^2 \cdot \left(\frac{k_{sED}}{h_D}\right)^{1/3} \cdot \left(\frac{H}{h_D}\right)^3 \cdot L_{ED}, \quad (14)$$

where L_{ED} is the length of the section between profiles E and D and k_{sED} is hydraulic roughness of outflow channel bed between profiles E and D.

Modular limit expressed by the ratio of H_{f0}/H is then determined from Bernoulli's equation

$$\frac{H_{f0}}{H} = 1 - \frac{h_{zUC}}{H} - \frac{h_{zCT}}{H} - \frac{h_{zCE}}{H} - \frac{h_{zE}}{H} - \frac{h_{zED}}{H} . \tag{15}$$

After Equation (8) is substituted in equations for individual head losses (6), (7), (12), (13) and (14) and after they are substituted in Equation (15), and under the simplifying assumption that $h_D = P_D + h_T$ (idealised flow in outflow channel is uniform and water level upstream and downstream the local loss is identical), equation for direct determination of H_{f0}/H is obtained

$$\frac{H_{f0}}{H} = \frac{h_C}{H} + \frac{2^2}{3^3}\cdot\alpha_C\cdot C_d^2\cdot\left(\frac{H}{h_C}\right)^2 - \frac{1}{2^4}\cdot\frac{\left\{\left[1+\frac{2^6}{3^3}\cdot C_d^2\cdot\left(\frac{H}{h_C}\right)^3\right]^{1/2}-3\right\}^3}{\left[1+\frac{2^6}{3^3}\cdot C_d^2\cdot\left(\frac{H}{h_C}\right)^3\right]^{1/2}-1}\cdot\frac{h_C}{H}$$

$$-\left(\frac{2}{3}\right)^3\cdot\left(\frac{C_d}{C_k}\right)^2\cdot\left(\frac{k_{sCE}}{h_C}\right)^{1/3}\cdot\left(\frac{H}{h_C}\right)^3\cdot\frac{2^{20/3}}{\left\{\left[1+\frac{2^6}{3^3}\cdot C_d^2\cdot\left(\frac{H}{h_C}\right)^3\right]^{1/2}+1\right\}^{10/3}}\cdot\left(\frac{L}{H}-2.7\right)$$

$$-\frac{2^4}{3^3}\cdot\alpha_D\cdot C_d^2\cdot\xi_E\cdot\left(\frac{H}{h_C}\right)^2\cdot\left\{\frac{1}{\left[1+\frac{2^6}{3^3}\cdot C_d^2\cdot\left(\frac{H}{h_C}\right)^3\right]^{1/2}-1}-\frac{1}{2\cdot\frac{P_D}{H}\cdot\frac{H}{h_C}+\left[1+\frac{2^6}{3^3}\cdot C_d^2\cdot\left(\frac{H}{h_C}\right)^3\right]^{1/2}-1}\right\}^2$$

$$-\left(\frac{2}{3}\right)^3\cdot\left(\frac{C_d}{C_k}\right)^2\cdot\frac{1}{\left(\frac{P_D}{k_{sED}}+\frac{h_C}{2\cdot k_{sED}}\cdot\left\{\left[1+\frac{2^6}{3^3}\cdot C_d^2\cdot\left(\frac{H}{h_C}\right)^3\right]^{1/2}-1\right\}\right)^{1/3}}\cdot\frac{1}{\left(\frac{P_D}{H}+\frac{h_C}{2\cdot H}\cdot\left\{\left[1+\frac{2^6}{3^3}\cdot C_d^2\cdot\left(\frac{H}{h_C}\right)^3\right]^{1/2}-1\right\}\right)^3}\cdot\frac{L_{ED}}{H} \tag{16}$$

The equation includes coefficients and ratios that need to be quantified. Measurements show that kinetic energy coefficient in profile C is $\alpha_C = 1.03$ (Hager and Schwalt, 1994), simplified $\alpha_C = 1.0$; in profile D it is $\alpha_D = 1.11$ (Zubík, 2006), simplified $\alpha_D = 1.1$. 10% change in the value of α_D results in the change in H_{f0}/H by maximum 3%. $\xi_E = 1$ applies for vertical downstream weir face (Brater et al., 1996). In the range of $5 < k_s/h < 500$, $C_k = 8.1$ (García, 2008) is considered. Values of k_{sCE} and k_{sED} are determined according to the surface material (Idel´chik, 1966). For smooth surfaces (considered below) and $h \geq 0.06$ m, $k_s = 0.00013$ m is used. For $h \geq 0.06$ m, $0.12 \leq h/L \leq 0.30$ and $h/b \leq 0.5$, C_d is defined from equation (Zachoval, 2015; Zachoval et al., 2014) ($R^2 = 0.98$):

$$\text{for } 0.10 \leq \frac{h}{P_U} < 0.52 \text{ it means } C_d = 0.845 , \tag{17a}$$

$$\text{for } 0.52 \leq \frac{h}{P_U} < 7.0 \text{ it means } C_d = 0.038\cdot\ln\frac{h}{P_U} + 0.87 . \tag{17b}$$

Relation between C_d and h/P_U with values measured by many authors is shown in Fig. 2 (Zachoval et al., 2014a).

Upon the measurement (Zachoval, 2015), the h_C/H ratio for $h \geq 0.06$ m, $0.08 \leq h/L \leq 0.30$ and $h/b \leq 0.5$ ($R^2 = 0.98$) is:

$$\text{for } 0.10 \leq \frac{h}{P_U} < 0.52 \text{ it means } \frac{h_C}{H} = 0.47 , \tag{18a}$$

$$\text{for } 0.52 \leq \frac{h}{P_U} < 2.5 \text{ it means } \frac{h_C}{H} = 0.038\cdot\ln\frac{h}{P_U} + 0.495 . \tag{18b}$$

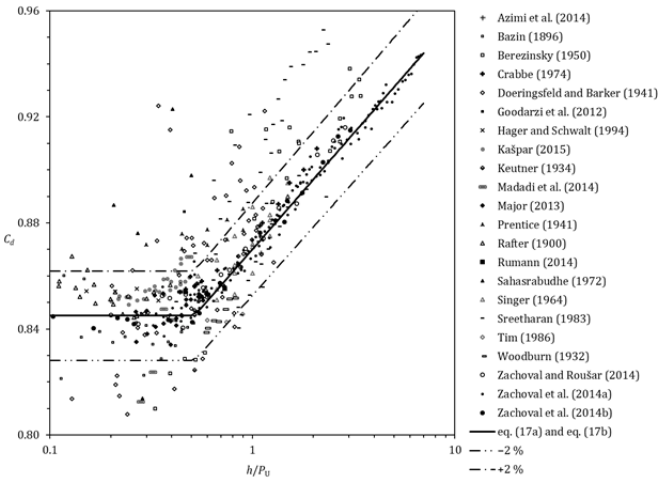

Fig. 2. Relation between C_d and h/P_U for $h \geq 0.06$ m, $0.10 \leq h/L \leq 0.30$, $h/b \leq 0.5$.

Using the above method, modular limit can be determined for any full-width sharp-edged broad-crested rectangular weir in scope of validity of empirical Equations (17) and (18). To verify validity of the above derivation, data acquired through experiments are necessary. As they had not been measured in the required range, experiments were carried out. The experiments are described in section EXPERIMENTS; verification is in section EVALUATION.

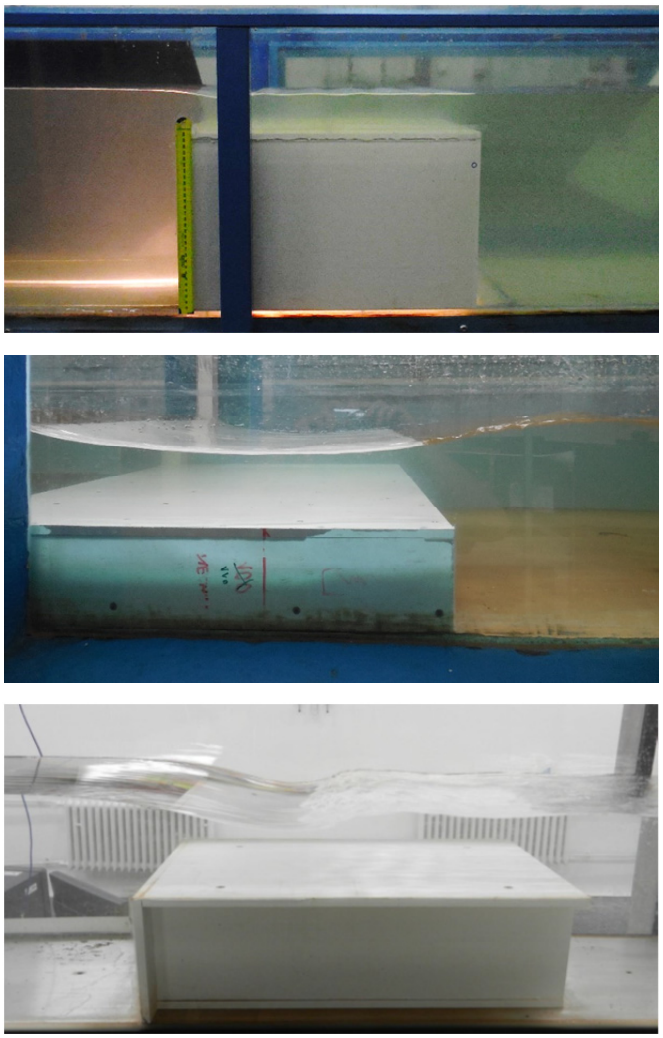

Fig. 3. From the top: channel BUT 0.5 with weir $P = 0.300$ m, channel BUT 1 with weir $P = 0.113$ m, channel SUTB with weir $P = 0.150$ m.

To justify the use of the simplifications described above, the significance of individual head losses on total head loss had to be analysed. The analysis is presented in section EVALUATION.

Submergence coefficient

The submergence coefficient, C_f, is derived by modifying Villemonte's application of the principle of superposition (Villemonte, 1947). The modification consists in relating H and H_f to the total submergence head at modular limit (not to the weir crest level), i.e. to H_{f0}. The discharge given by $H - H_{f0}$ is then

$$Q_u = C_d \cdot \left(\frac{2}{3}\right)^{3/2} \cdot g^{1/2} \cdot b \cdot \left(H - H_{f0}\right)^{3/2} \tag{19}$$

and discharge given by $H_f - H_{f0}$ is

$$Q_d = C_{dd} \cdot \left(\frac{2}{3}\right)^{3/2} \cdot g^{1/2} \cdot b \cdot \left(H_f - H_{f0}\right)^{3/2}, \tag{20}$$

where C_d and C_{dd} are discharge coefficients. C_f is determined by discharge ratio in submerged flow conditions, $Q = Q_u - Q_d$, and discharge in free flow conditions, Q_u; after substitution in Equations (19) and (20)

$$C_f = \frac{Q}{Q_u} = \left(1 - \frac{Q_d}{Q_u}\right)^{C_m} = \left(1 - \frac{C_{dd} \cdot \left(H_f - H_{f0}\right)^{3/2}}{C_d \cdot \left(H - H_{f0}\right)^{3/2}}\right)^{C_m}. \tag{21}$$

Provided that $C_{dd}/C_d = C$, the equation is reduced to

$$C_f = \left[1 - C \cdot \left(\frac{H_f - H_{f0}}{H - H_{f0}}\right)^{3/2}\right]^{C_m}, \tag{22}$$

where C is a proportional coefficient and C_m a power law exponent which need to be determined through an experiment.

EXPERIMENTS

Experiments were carried out in three channels (flumes) (Table 2) with the channel width marked B and active length of the channel marked l. The channels were named according to the institution where they are located: first and second channels in Laboratory of Water Management Research in the Institute of Water Structures at the Faculty of Civil Engineering at the Brno University of Technology (BUT 0.5 and BUT 1), the third one in the Department of Hydraulic Engineering at the Faculty of Civil Engineering at the Slovak University of Technology in Bratislava (SUTB). The channels were provided with transparent side walls made of glass (BUT 1 and SUTB) or polymethylmethacrylate (PMMA) (BUT 0.5). Horizontal channel beds were made of PMMA (BUT 0.5), polished concrete (BUT 1) and stainless steel (SUTB). All channels were equipped with water recirculation.

Full-width sharp-edged broad-crested rectangular weirs (Fig. 3) $B = b$, length L in the direction of flow and height $P = P_U = P_D$ (Table 3) above the channel bed were made of 0.010 m thick polyvinylchloride (PVC) boards with reinforcement ribs (to avoid deformation). The surface was smooth with sharp edges. The weirs in the channels were sealed by silicon sealant. Their position was chosen to ensure sufficiently long approach l_u and outflow l_d channel sections with developed velocity profile (Table 2).

The discharge Q (Table 3) was measured in the supply pipe by flow meters (Table 2); position of water level in outflow channel was set by adjustable tailgates (Table 2). Water level in approach channel in the distance of $3h$ in front of the upstream weir face and water level in outflow channel $10h$ after the downstream weir face (ISO 3846, 2008) were measured by needle gauges (Table 2). Due to the waves formed in the outflow channel, floating board of foam PVC was installed in front of the profile where water level was measured. Water temperature ranged from 18°C to 22°C. Range of measured heads, h, (Table 3) was chosen with respect to the requirements set in the definition of broad-crested weirs not affected by friction and surface tension. Detail information on channels, weirs and measurements can be found in publications listed in Table 3.

Modular limit was determined by means of polynomial approximation curve for $C_f = f\{H_f/H\}$ only in the case of submerged flow ($C_f < 1$). Extrapolation of the approximation curve up to $C_f = 1$ defined the modular limit H_{f0}/H. The method was suitable due to the sufficiently high number of measurements taken under submerged flow conditions.

To verify usability of results for all weirs, values of C_d under free flow conditions were analysed in the ranges of $0.10 \le h/L \le 0.30$, $h \ge 0.06$ m, $h/b \le 0.5$ (Fig. 2). The analysis proved that within the determination uncertainty, values of C_d do not depend on used values of b and L but only on h/P pursuant to the recommendation by Zachoval et al. (2014a).

Table 2. Channel parameters.

ID	l (m)	$B = b$ (m)	l_u (m)	l_d (m)	Flow meter, uncertainty at 95% confidence interval	Tailgate	Gauge, resolution (mm)
BUT 0.5	6	0.503	4.0	1.5	electromagnetic, ±0.2%	needle	point, 0.5
BUT 1	12	1.003	8.0	3.4	V-notch weir, ±1.0% to ±1.6%	sluice	point, 0.1
SUTB	7.5	0.409	5.5	1.5	electromagnetic, ±0.2%	flap	point, 0.1

Table 3. Weir parameters and range of measured quantities (N number of measurements).

ID	L (m)	$P = P_U = P_D$ (m)	Q (m³/s)	h (m)	h/L	h/P	h/b	N	Reference
BUT 0.5	0.5	0.051, 0.100, 0.150, 0.200, 0.250, 0.300	0.010–0.065	0.060–0.220	0.11–0.44	0.20–4.14	0.11–0.44	234	Zachoval and Roušar (2014)
BUT 1	0.6	0.052, 0.113, 0.254, 0.603	0.022–0.112	0.061–0.285	0.10–0.48	0.10–4.03	0.06–0.28	193	Zachoval et al. (2014a)
SUTB	0.5	0.150	0.022–0.038	0.109–0.244	0.22–0.49	0.73–1.63	0.27–0.6	14	Rumann (2014)

EVALUATION

Modular limit

Visual observation and photographic documentation of the experiments under modular limit conditions implied that the water level on the weir crest mainly depends on the ratios of h/L and h/P. Undular hydraulic jump appears on the crest. If $h/L = 0.1$, three wave peaks are formed; if $h/L = 0.4$, one peak is formed. Formation of the undular hydraulic jump complies with the observations and measurements by Berezinskij (1950), Hager and Schwalt (1994) and Wols (2005).

Verification of applicability of Equation (16) to determine H_{f0}/H on the basis of the h/P ratio is illustrated in Fig. 4 for smooth surfaces. The graph includes values from the actual experimental research (Rumann (2014) – SUTB; Zachoval and Roušar (2014) – BUT 0.5; Zachoval et al. (2014) – BUT 1) and values defined by other authors (Halliwell and Hill (1967) specified in Markland et al. (1967)) in the ranges of $0.10 \le h/L \le 0.30$, $h \ge 0.06$ m and $h - h_f > 0.01$ m. For comparison purpose, curves defined by calculation from Equation (16) showing the limits of h/L for the approximately medium head over the weir measured in experiments for $h = 0.1$ m are depicted. The graph implies that with respect to measuring uncertainty, Equation (16) provides sufficiently accurate results for majority of the measured data within the entire range, i.e. $0.10 \le h/P \le 3.0$.

It is not possible to verify Equation (16) upon measurements for $P_U \ne P_D$, different relative roughness and different kinetic energy coefficients as there are no measured data. In these cases, the equation is not verified. Provided it could also be used for $P_U \ne P_D$, the effect of certain quantities and ratios may be analysed as shown in Fig. 5. Modular limits are illustrated by 6 curves. The curves for $h/P_U = 0.52$ refer to upper limit of high weirs where the values of C_d and h_C/H are independent of the h/P_U (17a, 18a). Curves for $h/P_U = 2.5$ are limit curves for determination of h_C/H (18b). The values for $h/L = 0.1$ and $h/L = 0.3$ define the range in which the value of C_d is independent of the h/L ratio. To express the scale effect caused by friction and surface tension, minimum head over weir not affected by friction and surface tension was defined to be $h = 0.06$ m (ISO 3846, 2008; Zachoval et al., 2014); maximum value for practical use was set to $h = 10$ m. The graph in Fig. 5 implies that all the above effects in ranges $0 \le h/P_D \le 1$, $0 \le h/P_U \le 2.5$, $0.10 \le h/L \le 0.30$, $h/b \le 0.5$ and for smooth surfaces are negligible, and can be substituted by a single curve. In the case of $h/P_D > 1$, the effects are different and cannot be neglected.

Equation (16) is applicable only to broad-crested weirs in the range of $0.10 \le h/L \le 0.30$. The Equation (16) cannot be used for other ranges, as the flow is not described sufficiently. To justify the use of the adopted simplification when deriving the Equation (16), graph of the relation between the relative individual head loss h_{zi}/h_z and h/P_D for smooth surfaces and for limit cases was elaborated. Two limit cases were specified form Fig. 5 as approximate envelope of all curves in Fig. 5: $h/P_U = 2.5$, $h/L = 0.3$, $h = 10$ m and $h/P_U = 0.52$, $h/L = 0.1$, $h = 0.06$ m. The relation is presented in Fig. 6. The graph shows that when h/P_D increases, the values of h_{zUC}/h_z, h_{zCT}/h_z, h_{zCE}/h_z a h_{zED}/h_z increase but the ratio of h_{zE}/h_z decreases. Within the sum, two individual relative losses, h_{zUC}/h_z and h_{zE}/h_z, are dominant (67% to 98%). The individual significance of other relative losses is relatively small, so the adopted simplifications can be considered acceptable for this case.

Practical use of Equation (16) is difficult, because the formula is very complicated. However, a simple, generally applicable equation with high accuracy cannot be found. Simplification of the equation results in limited applicability range. For a common case of real application: smooth surfaces, $P_U = P_D$, $0.10 \le h/L \le 0.30$, $h/b \le 0.5$ and range $0 \le h/P \le 3.5$, the Equation (16) can be approximated by the following formula

$$\frac{H_{f0}}{H} = 0.71 + 0.18 \cdot \left(\arctan \frac{h}{P} \right)^{0.71}, \tag{23}$$

where the coefficient of determination is $R^2 = 0.94$ for the data measured by us (Table 3). Equation (23) is (if Equation (16) is valid) applicable also for $P_U \ne P_D$ for ranges $0 \le h/P_D \le 1$, $0 \le h/P_U \le 2.5$, $0.10 \le h/L \le 0.30$, $h/b \le 0.5$ and for smooth surfaces (P in the Equation (23) is replaced by P_D). Curve for Equation (23) is shown in both Fig. 4 and Fig. 5 which imply good agreement with Equation (16) as well as the measured data.

Submergence coefficient

The $C_m = 2/5$ and the $C = 1$ were determined by the method of least squares (while respecting uncertainties of measurement) and with use of Equation (23) from all measured data fulfilling the conditions $0.1 \le h/P \le 2.5$, $0.10 \le h/L \le 0.30$, $h/b \le 0.3$, $h \ge 0.06$ m and $h - h_f \ge 0.01$ m. The submergence coefficient, C_f, for $P_U = P_D$ is then

$$C_f = \left[1 - \left(\frac{H_f - H_{f0}}{H - H_{f0}} \right)^{3/2} \right]^{2/5}. \tag{24}$$

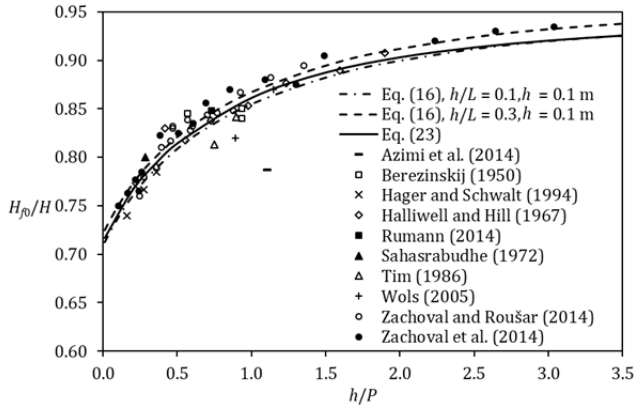

Fig. 4. Dependence of H_{f0}/H and h/P; data complying with requirements on $P_U = P_D$, $h \geq 0.06$ m, $0.10 \leq h/L \leq 0.30$, $h/b \leq 0.5$, $h - h_f > 0.01$ m and smooth surfaces.

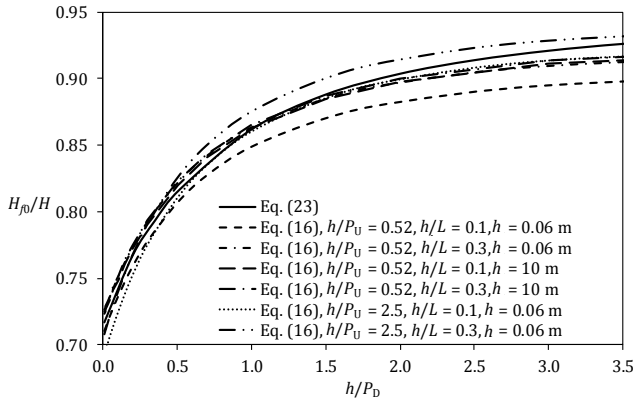

Fig. 5. Dependence of H_{f0}/H and h/P_D for smooth surfaces.

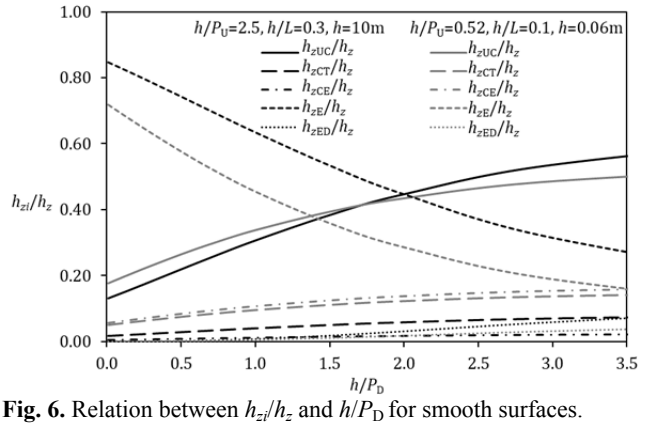

Fig. 6. Relation between h_{zi}/h_z and h/P_D for smooth surfaces.

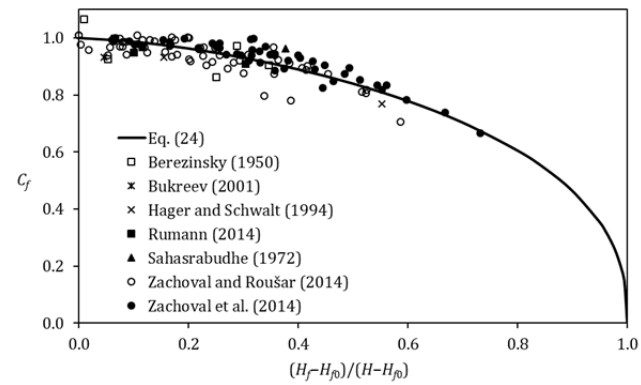

Fig. 7. Dependence of C_f on $(H_f - H_{f0})/(H - H_{f0})$, measured data.

The measured data and Equation (24) were plotted on a graph in Fig. 7. The graph shows good agreement (with respect to uncertainties in measuring small difference $h - h_f$) with the data measured within the range $0 \leq (H_f - H_{f0})/(H - H_{f0}) < 0.7$. For $P_U \neq P_D$, the exponent C_m, and coefficient C could not have been determined due to the lack of measured data.

Comparisons of the calculated coefficients by Equation (24) $C_{f\,\text{Eq. (24)}}$, by Azimi et al. (2014) equation $C_{f\,Azimi\ et\ al.\ (2014)}$, by the Berezinsky (1950) equation $C_{f\,Berezinsky\ (1950)}$, by the Hager and Schwalt (1994) equation $C_{f\,Hager\ and\ Schwalt\ (1994)}$ and computed coefficients from measurement C_f are shown in the Fig. 8 to Fig. 11. The figures imply that the C_f is computed most accurately by Equation (24), Azimi et al. (2014) computed the values inaccurately, Berezinsky (1950) computed the values relatively accurately in the whole range of measured data, and Hager and Schwalt (1994) computed the values relatively accurately in the range of $0.8 < C_f \leq 1.0$. In Fig. 12, comparison of the coefficients calculated by the Villemonte equation with $C = 1.18$ and $C_m = 0.14$ determined by the method of least squares $C_{f\,Villemonte}$ with the C_f is shown. The computed values are relatively accurate only in the range of $0.85 < C_f \leq 1.00$. Consequently, the original formula of Villemonte equation is less suitable for broad-crested weirs.

Method of determining the discharge

Recommended method of determination of the discharge, Q, for an overflow with identical heights of weir faces $P_U = P_D$ and smooth surfaces is:

- Measure the quantities P, h, h_f, L, b and define α_U, α_D (estimate or from measurement). Calculate the ratios h/L, h/P, h/b.
- Verify the applicability of relations for the calculation where $h \geq 0.06$ m, $0.1 \leq h/P \leq 3.0$, $0.10 \leq h/L \leq 0.30$, $h/b \leq 0.33$ must be met and the uncertainty of determining the difference between water levels in profiles U and D must be lower than the maximum permissible uncertainty of Q determination.
- Calculate H_{f0}/H from Equation (23) and C_d from Equations (17). By iteration with use of Equations (1, 2, 3), calculate Q for free flow and then H_f/H. If $H_f/H < H_{f0}/H$, free flow conditions apply and the calculation is completed; if not, the conditions comply with submerged flow and the following step is to be taken.
- Determine Q by iteration with use of Equations (1, 2, 3, 17, 23, 24).

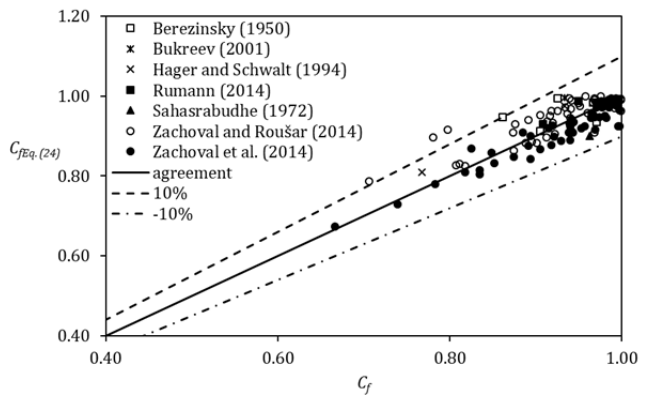

Fig. 8. Graph of agreement between $C_{f\,Eq.\ (24)}$ and C_f.

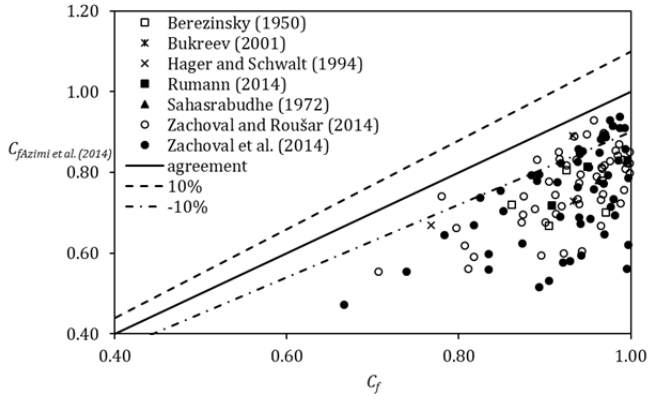

Fig. 9. Graph of agreement between $C_{f\,Azimi\ et\ al.\ (2014)}$ and C_f.

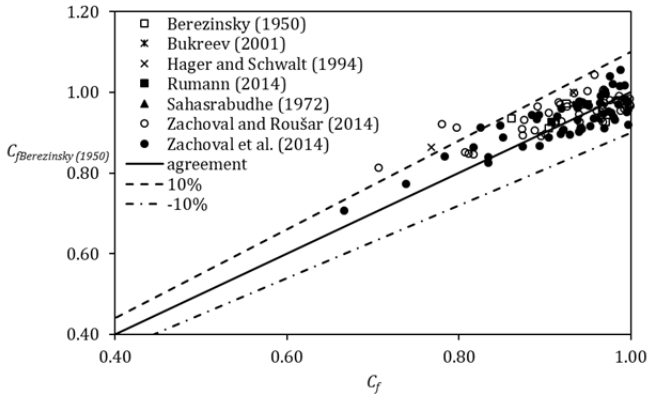

Fig. 10. Graph of agreement between $C_{f\,Berezinsky\ (1950)}$ and C_f.

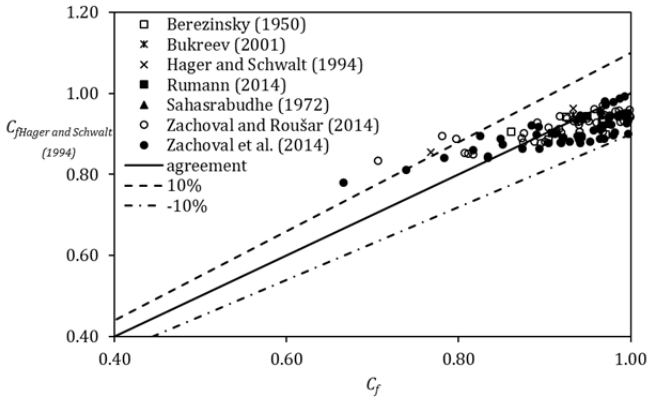

Fig. 11. Graph of agreement between $C_{f\,Hager\ and\ Schwalt\ (1994)}$ and C_f.

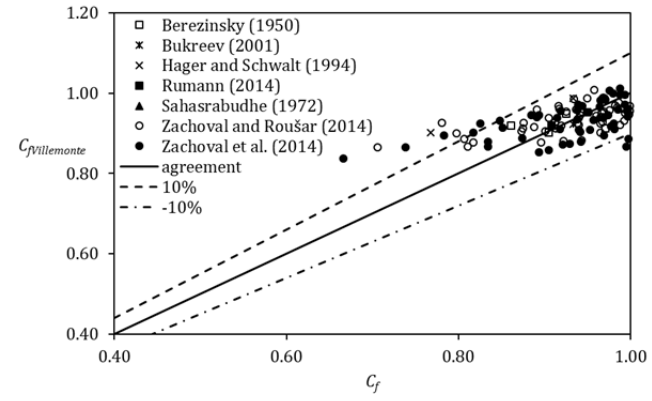

Fig. 12. Graph of agreement between $C_{f\,Villemonte}$ and C_f.

CONCLUSION

The article introduces derivation of the equation to determine modular limit expressed by the H_{f0}/H ratio for full-width sharp-edged broad-crested rectangular weir in the range $0.10 \leq h/L \leq 0.30$ situated in a channel of rectangular cross-section without the effect of friction on side walls and surface tension (16). After analysing the practically applicable ranges and for the case of identical heights of weir faces $P_U = P_D$, the equation was replaced by simple and sufficiently accurate empirical Equation (23) which is, in limited range, also probably applicable (is not verified by measured data) for $P_U \neq P_D$. The article also presents derivation of the equation to determine submergence coefficient, C_f, with empirically defined exponent C_m valid only in the case of $P_U = P_D$. The result is a system of equations describing both free and submerged flow over weir. The described system of equations enables a more accurate calculation of the discharge than those of other above mentioned authors. In the range $0.65 < C_f \leq 1.00$, the error in C_f definition amounts to ±10%.

Considerable extent of the experimental research enabled verification and simplification of the derived equation for modular limit and determination of the exponent for submergence coefficient. Within the experimental research, effort was made to measure the data as accurately as possible for the entire range of broad-crested weirs where the discharge coefficient for free flow is independent of the h/L ratio.

The research implied some important knowledge. Determination of modular limit is dependent on the used method (extrapolation of the approximation curve, agreed value of the change of water surface level in profile U etc.) which affects the evaluation by considerable uncertainty. At modular limit, water level in the outflow channel undulates, which is why mean value shall be considered with respect to both time and area (within the wave length). With the increase in value of the $(H_f - H_{f0})/(H - H_{f0})$ ratio, the uncertainty of determining the difference of water levels at profiles U and D increases; analysis of its effect is therefore recommended for each case.

Acknowledgement. This study was supported by project FAST-S-14-2203 Characteristics of submergence of low rectangular broad-crested weirs and project FAST-S-16-3757 Increasing of safety and reliability of selected hydrotechnical structures.

REFERENCES

Azimi, A.H., Rajaratnam, N., Zhu, D.Z., 2014. Submerged flows over rectangular weirs of finite crest length. J. Irrig. Drain. Eng., 140, 5, 06014001, 1–12.

Bazin, H., 1896. Expériences nouvelles sur l´écoulement en déversoir. 5 article. Annales des ponts et chaussées. Mémoires et documents relatifs à l'art des constructions et au service de l'ingénieur. 2 semestre, Gallica, Paris, pp. 645–731.

Berezinsky, A.P., 1950. Carrying Capacity of the Broad-Crested Weir. Vodgeo, Moscow. (In Russian.)

Bos, M.G., 1984. Long-Throated Flumes and Broad-Crested Weirs. Martinus Nijhoff/Dr W. Junk Publishers, Dordrecht.

Bos, M.G., 1989. Discharge Measurement Structures. Third revised edition. Publication 20. ILRI, Wageningen.

Brater, E.F., King, H.W., Lindell, J.E., Wei, C.Y., 1996. Handbook of Hydraulics. McGraw-Hill, New York.

Brownlie, W.R., 1981. Compilation of alluvial channel data: Laboratory and field. Report No. KH-R-43B. California Institute of Technology, Pasadena.

Bukreev, V.I., 2001. Undular jump in open-channel flow over a sill. Journal of Applied Mechanics and Technical Physics, 42, 4, 596–602.

Chanson, H., 2009. Current knowledge in hydraulic jumps and related phenomena. A survey of experimental results. European Journal of Mechanics B/Fluid, 28, 191–210.

Crabbe, A.D., 1974. Some hydraulic features of the square edged broad-crested weir. Water and Water Eng., 78, 10, 354–358.

Doeringsfeld, H.A., Barker, C.L., 1941. Pressure-momentum theory applied to the broad-crested weir. Trans. ASCE, 106, 1, 934–946.

García, M.H., 2008. Sedimentation Engineering: Processes, Measurements, Modelling, and Practice. ASCE, Reston.

Goodarzi, E., Farhoudi, J., Shokri, N., 2012. Flow characteristics of rectangular broad-crested weirs with sloped upstream face. J. Hydrol. Hydromech., 60, 2, 87–100.

Govinda Rao, N.S., Muralidhar, D., 1963. Discharge characteristics of weirs of finite-crest width. La Houille Blanche, 18, 5, 537–545.

Hager, W.H., Schwalt, M., 1994. Broad-crested weir. J. Irrig. Drain. Eng., 120, 1, 13–26.

Hager, W.H., 2010. Wastewater Hydraulics. Springer, Heidelberg.

Harrison, A.J.M., 1967. The streamlined broad-crested weir. Proc. ICE, 38, 4, 657–678.

Horton, R.E., 1907. Weir Experiments, Coefficients, and Formulas. U.S.G.S., Washington.

Idel´chik, J.E., 1966. Handbook of Hydraulic Resistance. Coefficients of Local Resistance and of Friction. Israel Program for Scientific Translations, Jerusalem.

ISO 3846, 2008. Liquid flow measurement in open channels by weirs and flumes. Rectangular broad-crested weirs. IOS, Geneva.

Kašpar, T., 2015. Influence of the weir width on a discharge coefficient of the broad crested weir. Batchelor thesis. Brno University of Technology, Brno, Czech Republic. (In Czech.)

Keutner, C., 1934. Strömungsvorgänge an breitkronigen wehrkörpern und an einlaufbauwerken. Der Bauingenieur, 15, 366–371.

Madadi, M.R., Dalir, A.H., Farsadizadeh, D., 2014. Investigation of flow characteristics above trapezoidal broad-crested weirs. Flow Measurement and Instrumentation, 38, 139–148.

Major, J., 2013. Influence of upstream face inclination of broad-crested weir on discharge coefficient. Bachelor thesis. Brno University of Technology, Brno, Czech Republic. (In Czech.)

Markland, E., Abbott, M.B., Montes, S.S., Allen, J., Smith, C.D., Manning, R., Jaeger, C., Herschy, R.W., Halliwell, A.R. and Hill, J.A., Engel, F.V.A., Williams, J.M., Bunt, E.A., Hall, G.W., 1967. Discussion of the streamlined broad-crested weir. ICE Proc., 38, 657–678.

Montes, J.S., Chanson, H., 1998. Characteristics of undular hydraulic jumps: experiments and analysis. J. Hydr. Eng., 121, 2, 192–205.

Nikolov, N.A., Minkov, I.N., Dimitrov, D.K., Mincheva, S.K., Mirchev M.A., 1978. Hydraulic calculation of a submerged broad-crested weir. Hydrotechnical Construction, 12, 6, 631–634.

Noor Afzal, Bushra, A., Abu Seena, 2011. Analysis of turbulent hydraulic jump over a transitional rough bed of a rectangular channel: universal relations. J. Eng. Mech., 137, 12, 835–845.

Pavlovskij, N.N., 1937. Hydraulic Reference Book. ONTI, Leningrad. (In Russian.)

Rafter, G.W., 1900. On the flow of water over dams. Report on special water-supply investigation. Part II. Appendix No. 16. Transaction of ASCE, 44, 220–398.

Rumann, J., 2014. Submergence characteristic of low rectangular broad-crested weirs – validation measurement. Slovak University of Technology in Bratislava, Bratislava. (In Slovak.)

Sahasrabudhe, S.J., 1972. Discharge characteristics of submerged broad crested weirs. M.E. thesis. University of Rookee, Rookee.

Singer, J., 1964. Square-edged broad-crested weir as a flow measurement device. Water and Water Eng., 28, 820, 229–235.

Skogerboe, G.V., Hyatt, M.L., Austin, L.H., 1967. Design and Calibration of Submerged Open Channel Flow Measurement Structures: Part 4 – Weirs. Utah State University, Logan.

Sreetharan, P.M., 1983. Analytical and experimental investigation of flow measurement by long-based weirs in the rectilinear and curvilinear ranges. PhD thesis. The Hatfield Polytechnic, Hatfield, Hertfordshire, England.

Stevens, J.C., Wilm, H.G., Nelidov, I.M., Hackney, J.W., Prentice, T.H., Bakhmeteff, B.A., Curtis, D.D., Rohwer, C., Hedberg, J., 1941. Discussion of "Doeringsfeld, H.A., Barker, C.L., 1941. Pressure-momentum theory applied to the broad-crested weir". Transactions of the ASCE, 106, 1, 947–967.

Tim, U.S., 1986. Characteristics of some hydraulics structures used for flow control and measurement in open channels. PhD thesis. Concordia University, Montreal.

USACE, 1977. Hydraulic Design Criteria. Low-Monolith Diversion, Discharge Coefficients. USACE, Vicksburg.

Villemonte, J.R., 1947. Submerged-weir discharge studies. Eng. News Record, 867, 54–57.

Wols, B.A., 2005. Undular hydraulic jumps. M.Sc. Thesis. Delft University of Technology, Delft.

Woodburn, J.G., 1932. Tests of broad-crested weirs. Transactions of the American Society of Civil Engineers, 96, 1, 387–416.

Zachoval, Z., 2015. Broad-crested weirs with rectangular control section. Brno University of Technology, Brno.

Zachoval, Z., Mistrová, I., Roušar, L., Šulc, J., Zubík, P., 2012a. Zone of flow separation at the upstream edge of a rectangular broad-crested weir. J. Hydrol. Hydromech., 60, 4, 288–298.

Zachoval, Z., Pařílková, J., Roušar, L., 2012b. Velocity measurements in front of rectangular broad-crested weir. In: Chára, Z., Klaboch, L. (Eds.): Proc. 20th Symposium on Anemometry (Holany-Litice, Czech Republic 2006). Institute of Hydrodynamics ASCR, Prague, pp. 81–86. (In Czech.)

Zachoval, Z., Roušar, L., 2014. Bed load transport over rectangular broad-crested weir. Brno University of Technology, Brno. (In Czech.)

Zachoval, Z., Kněblová, M., Roušar, L., Rumann, J., Šulc, J., 2014a. Discharge coefficient of a rectangular sharp-edged broad-crested weir. J. Hydrol. Hydromech., 62, 2, 145–149.

Zachoval, Z., Roušar, L., Major, J., 2014b. Characteristics of submergence of low rectangular broad-crested weirs. Brno University of Technology, Brno. (In Czech.)

Zubík, P., 2006. PIV and LDA flow parameters measurement in the water channel with high negative step. In: Chára, Z., Klaboch, L. (Eds.): Proc. 20th Symposium on Anemometry (Holany-Litice, Czech Republic 2006). Institute of Hydrodynamics ASCR, Prague, pp. 105–114. (In Czech.)

Received 11 June 2018
Accepted 12 July 2019

NOMENCLATURE

b	weir width (m)
B	channel width (m)
C	proportional coefficient
C_d	discharge coefficient
C_{dd}	discharge coefficient
C_f	submergence coefficient
C_k	coefficient
C_m	power law exponent
C_v	approach velocity coefficient
Fr	Froude number
g	gravitational acceleration (m/s^2)
h	head, depth (m)
h_f	submergence head (m)

h_z head loss (m)
H total head (m)
H_f total submergence head (m)
i slope
k_s hydraulic roughness (m)
l length (m)
L weir length in direction of flow (m)
N number of measurements
P weir height (m)
q specific discharge (m^2/s)
Q discharge (m^3/s)
R^2 coefficient of determination
v mean velocity at a cross-section (m/s)
α kinetic energy coefficient
ξ minor loss coefficient

Subscripts:
d downstream
u upstream
0 modular limit
U, C, T, E, D profiles